Strength Grading of Northern Hardwood Species for Structural Engineered Wood Products: Identification of the Relevant Indicating Properties

Alexandre Morin-Bernard,[a,b,*] Pierre Blanchet,[a,b] Christian Dagenais,[a,b,c] and Alexis Achim [b]

Strength grading of hardwoods is required for their use in structural engineered wood products. However, hardwood strength grading is considerably less developed than it is for softwood species. Previous study has shown that white ash and yellow birch are promising species for the manufacture of glued-laminated timber. However, no dedicated strength grading procedure for hardwoods is available in Canada. This study aimed to identify the relevant properties for predicting the ultimate tensile strength of the investigated species. A model selection approach allowed the identification of the best performing models, comparison of each species, and determination of the relative impact of the indicating properties. The indicating properties included in the final models were the density of the specimens, the dynamic modulus of elasticity, the sine of the maximum local grain deviation (SGD_{max}), and the knot area index (*KAI*), which was derived from the knot area ratio. The final models revealed important differences between the two species that indicated that they should be graded separately to ensure the most efficient resource utilization. The coefficients of determination between the actual and model predicted ultimate tensile strength (UTS) were 0.82 for white ash and 0.78 for yellow birch.

Keywords: Engineered wood products; Glued-laminated timber; Hardwood strength grading; Characteristic properties; Northern hardwood species; Ultimate tensile strength; Dynamic modulus of elasticity

*Contact information: a: NSERC Industrial Chair on Eco-responsible Wood Construction, Université Laval, 2425 rue de la Terrasse, Quebec, G1V 0A6, Canada; b: Renewable Materials Research Centre, Université Laval, 2425 rue de la Terrasse, Quebec, G1V 0A6, Canada; c: FPInnovations, 1055 rue du P.E.P.S, Quebec, G1V 4C7 Canada; *Corresponding author: alexandre.morin-bernard.1@ulaval.ca*

INTRODUCTION

In the last few decades, there has been a renewed interest in the use of hardwoods in construction (Green *et al.* 1994; Erickson and Ross 2005; Aicher *et al.* 2014). Their availability, impressive mechanical properties, and distinctive appearance are among the main factors driving the development of new structural engineered wood products from various broadleaf species. The value of the timber from hardwood species and its potential for use in engineered wood products depends on the knowledge of its mechanical properties and behavior under load. However, the inherent variability associated with the structure and anatomical features of hardwoods causes uncertainty with respect to their mechanical properties. The types of cells, their proportion, the relative amount of their chemical constituents, and the nature and abundance of the strength-reducing defects are highly

variable between species, within the individuals of a given species, and even in a single tree (Panshin and Zeeuw 1970; Ridley-Ellis *et al.* 2016).

In engineering applications, this uncertainty is managed *via* design approaches that consider the natural variability of the material. Consideration of the 5th percentile level from the normal distribution of the lumber properties (also called characteristic properties) in the design calculations is a widespread practice. However, the variability is so large that the establishment of characteristic properties applicable to all hardwoods, or even to a single species, would lead to inefficient utilization of the raw material (Ravenshorst 2015). The strength grading process allows segregation of the timber in groups with the same strength properties, which allows for more efficient and economical use of the resource. For engineered wood products, such as glued-laminated timber (glulam), grading the lumber allows the identification and selection of the strongest material in the most solicited portions of the beam's cross section.

The strength grading process is based on the measurement of various parameters called indicating properties (IP), which affect the strength of timber and can be measured nondestructively (Erickson and Ross 2005; Schlotzhauer *et al.* 2019). The slope of grain, knots, density, and modulus of elasticity are among the most common characteristics measured for the strength grading of lumber. The influence of the slope of grain stems from the orthotropic nature of the wood material, which possesses independent mechanical properties in its three different axes, namely longitudinal, tangential, and radial. Wood is the strongest in the longitudinal axis, when a load is applied parallel to the direction of the wood fibres, vessels, or tracheids (Bodig and Jayne 1982; Ross 2010). However, in lumber this is rarely achieved. The growth conditions and structural features of the trees as well as the sawing pattern of the boards can result in lumber pieces in which the grain in not parallel to the longitudinal axis; this presents what is called slope of grain or grain deviation. Since the wood material is considerably weaker when the load is applied perpendicular to the grain, any deviation of the grain from the longitudinal axis reduces the strength of the lumber. This relationship has been studied and can be approximated using the Hankinson equation (Bodig and Jayne 1982; Ross 2010; Ravenshorst *et al.* 2019).

Knots are the remains of branches that were more or less perpendicular to the longitudinal axis of the tree trunk. In lumber, knots are considered to reduce the effective cross section and to cause discontinuity of the wood's oriented structure. The distortion of the fibres around the knot generates stress concentrations, which is directly related to the proportion of the cross section occupied by the knot (Ross 2010; Ravenshorst 2015). In addition, knots have a larger impact on strength in axial tension than in bending (Green *et al.* 1999). The density of the wood material is also related to its strength. Theoretically, a higher density implies a higher amount of cell wall material per volume unit and therefore, a higher strength. However, this relationship is only evident in clear wood specimens and is considerably weaker when defects such as grain deviations or knots are present (Bendtsen and Youngs 1981; Ross 2010; Ravenshorst 2015). The modulus of elasticity, as a measure of the stiffness, is known to be a good predictor of timber bending strength (Ross 2010; Ravenshorst 2015). It is frequently used in conjunction with density as the basis of timber strength grading because those properties are together dependent on other properties, such as the presence of grain deviations and knots (Ravenshorst 2015).

Most grading methods can be classified as either visual or machine grading. Visual grading is based on characteristics that can be assessed visually, such as the position, dimensions, and number of knots, the slope of grain, and the presence of reaction wood, fissures, wane, or rot (Ravenshorst 2015; Ridley-Ellis *et al.* 2016). Visual grading was the

only available method until the 1960s, and since the 1990s, grading has been based on the large-scale testing of lumber (Galligan and McDonald 2000). However, a considerable margin for safety must be added to account for the limited precision of human evaluation and the uncertainty in the relationships between the visual characteristics and strength. Therefore, visual grading does not allow the most efficient utilization of the real properties of the timber. Machine strength grading is now well-established, and a variety of methods and equipment are available to measure properties that can or cannot be assessed visually. These properties include the modulus of elasticity, density, moisture content, and direction of the wood fibres (Galligan and McDonald 2000). Currently, most grading approaches rely on a combination of visual and machine-based methods (Niemz and Mannes 2012; Ehrhart *et al.* 2016a). For instance, machine stress rated lumber (MSR) is also graded visually, because adding knot information to the stiffness considerably improves the precision of the process (Bendtsen and Youngs 1981).

The structure and mechanical properties of hardwood species are more complex and more variable than softwoods (Panshin and Zeeuw 1970; Bollmus *et al.* 2017), so the grading process is essential for their use in structural applications. Strength grading of hardwoods is considerably less developed than it is for softwoods (Kovryga *et al.* 2019a; Weidenhiller *et al.* 2019), which is probably because the mechanical properties of hardwood are less predictable (Schlotzhauer *et al.* 2019). In Canada, the dominant use of hardwoods in decorative products has defined the grading method. Hardwood lumber is sawn in factory lumber rather than in dimension lumber and graded for its appearance rather than for its mechanical properties (NHLA 2019). Moreover, hardwood grading based on the tensile strength, which is relevant for tension laminations in glulam, is still in the early stages of development. Despite comprising the tensile strength classes for softwoods, European standard CEN EN 338 (2016) does not yet include tensile strength classes dedicated to hardwood species.

However, research efforts conducted in the United States in the early 1990s showed that the relationships between the mechanical properties of softwoods, on which current strength grading methods are based, also apply to hardwoods (Green *et al.* 1994). Compared to softwoods, most hardwood species have a higher ultimate tensile strength (UTS) for a given bending strength (MOR) and a higher bending strength for a given modulus of elasticity (MOE). Therefore, it may be overly conservative to use the softwood relationships (Green *et al.* 1994; Kovryga *et al.* 2019b) to predict the characteristic properties of hardwood species. Moreover, the mechanical properties of some hardwood species are difficult to predict (Weidenhiller *et al.* 2019), and the interrelationships between the indicating properties vary as a function of the species (Kovryga *et al*. 2019b).

Previous work has shown that white ash (*Fraxinus americana* L.) and yellow birch (*Betula alleghaniensis* Britt.) are promising species for the manufacture of glulam (Morin-Bernard *et al.* 2020). However, there is little scientific knowledge on the mechanical properties of these species, which are not currently strength graded in Canada. This study aimed to identify the most suitable indicating properties, measured by a combination of visual and machine grading methods, to predict the ultimate tensile strength of white ash and yellow birch timber, using a modelling approach. In addition, the relative impact of the IPs on their mechanical properties and their capacity to be subjected to a strength grading process was discussed. To our knowledge, this is the first study to establish the basis for an operational and industrially applicable tensile strength grading of the investigated species. This study was part of a broader project aiming to foster the use of northern hardwood species in structural engineered wood products

EXPERIMENTAL

Materials

Lumber from the investigated hardwood species was purchased from Goodfellow Inc. in Quebec, Canada. Boards were processed to lamellae with cross-sectional dimensions of 38 mm × 38 mm and a length of 1830 mm. The resulting samples consisted of lamellae that presented a wide range of strength-reducing defects and lamellae without knots or any other visible strength-reducing defects. When a knot or a major grain deviation was present, the lamella was sawn so that the worst defect was positioned in the central portion of the lamella within the test span. A total of 62 white ash and 55 yellow birch specimens were prepared and tested.

Methods

Measurement of indicating properties and non-destructive testing

The maximum local grain deviation, the maximum grain deviation on a length equivalent to the width of the specimen, and the average slope of grain in the 610 mm test span (middle third) were recorded on each face of the specimens. The average slope of grain on the four faces of the piece was derived from the measurements. Due to the difficulty of measuring the fiber direction in hardwoods, multiple methods were used. When a radial surface was present, the growth ring boundaries were used to determine the angle of the grain, as suggested by Koehler (1955). For less evident specimens, a magnifying glass, a scribe, and the pattern after tensile failure were used to ensure the accuracy of the measurements. Data relative to the knots were recorded using the concept of the Knot Area Ratio (*KAR*), which corresponds to the projection of the knot on the cross-sectional area of the piece. The width of the knot, measured on every face where it was visible, was taken as the distance between lines drawn parallel to the length of the board and enclosing the knot. Every specimen had only one knot within the test span.

The dynamic modulus of elasticity (MOE_{dyn}) was measured using a HM200 Director acoustic velocity tool (Fiber-gen Instruments Limited, Christchurch, New Zealand) on all lamellae. The velocity of the sound wave measured by the tool was used to calculate MOE_{dyn} with Eq. 1,

$$MOE_{dyn} = \rho V^2 \quad (1)$$

where ρ is the density (kg/m^3) and V is the acoustic wave velocity (km/s).

To confirm the suitability of the HM200 Director as a tool to measure the stiffness of hardwood lamellae, the apparent modulus of elasticity in third point bending was also measured on 17 white ash and 18 yellow birch specimens. The loading span of 813 mm and the test setup conformed to ASTM D4761 (2013). Equation 2 was used to calculate the apparent modulus of elasticity (MOE_{app}),

$$MOE_{app} = 23Pl^3 / 108bd^3\Delta \quad (2)$$

where P is the increment of applied load on the specimen (N), l is the span of flexure (mm), b is the width of the specimen (mm), d is the depth of specimen (mm), and Δ is the increment of deflection of the specimen (mm) when subjected to the applied load, P.

Generalized linear models were built with the data from the lamellae that was subjected to both dynamic and static MOE measurement to establish the relationship between the two methods of measurement.

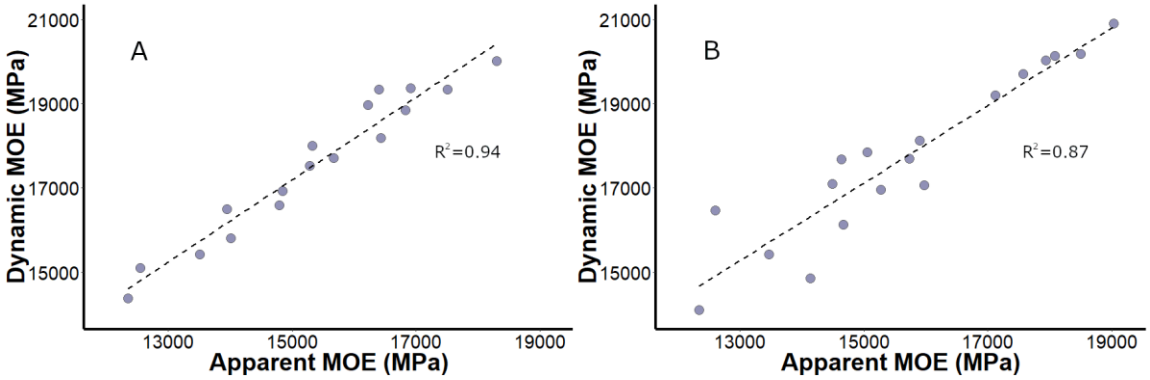

Fig. 1. The dynamic MOE values plotted against the apparent MOE measured in third point bending for white ash (A) and yellow birch (B)

The results in Fig. 1 are in line with the findings of Liu *et al.* (2014), who concluded that the MOE measured by dynamic techniques led to 5% to 20% higher values than that obtained from static measurement methods. In this study, the linear models relating the two methods showed a coefficient of determination of 0.94 for white ash and 0.87 for yellow birch. Coefficients derived from the linear models were used to assign an apparent modulus of elasticity value to the lamellae, for which the MOE was only assessed using the acoustic velocity tool. The relevant characteristics of the lumber tested in this study, including the strength-reducing defects, are shown in Table 1.

Table 1. Relevant Characteristics of the White Ash and Yellow Birch Lamellae

	White Ash	Yellow Birch
Number of Specimens	62	55
Density (kg/m³)		
Mean	712.7	717.9
Minimum	634.9	577.9
Maximum	798.5	794.0
SD	45.1	41.3
MOE_{app} (MPa)		
Mean	14,195	15,254
Minimum	8,806	11,035
Maximum	18,217	18,972
SD	2,342	1,857
Maximum Local Grain Deviation (°)		
Mean	26.3	26.6
Minimum	1.9	1.9
Maximum	71.7	62.4
SD	20.6	18.4
Knot Area Ratio (%)		
Mean	5.4	3.9
Minimum	0.0	0.0
Maximum	50.6	24.7
SD	11.0	6.1

Tension testing of the lumber

Tension testing of the specimens was realized with a hydraulic tension testing machine (Model 412; Metriguard Technologies Inc., Pullman, WA, USA) in accordance with ASTM D4761 (2013) for determination of axial strength in tension with a test span of 610 mm for a specimen width of 38 mm. The specimens were held in place by grips designed to minimize slippage. Samples were collected from each specimen after testing for determination of the moisture content (MC) in the vicinity of the failure zone. The UTS, MOE, and density values were adjusted to a 12% moisture content according to ASTM D1990 (2016).

Model development

To identify the explanatory variables that influence the UTS of the lamellae, a model selection process was performed using package AICcmodavg (Mazerolle 2019) within the R programming environment (R Foundation for Statistical Computing, version 3.6.3, Vienna, Austria). The procedure was realized separately for each of the species. Three groups of candidate models comprising a total of 20 models were built *a priori*. The first set comprised models with variables related to the characteristics measured by non-destructive testing of the lamellae, namely the dynamic MOE and density. The second group included the models involving variables linked to the defects recorded during the visual grading process. A third group was created with the models combining variables from the two aforementioned groups. In addition, an intercept-only model was included in the analysis. The variables included in the candidate models are presented in Table 2. Due to the nature of the relationship between the maximum grain deviation and UTS, a transformation was required. Variable SGD_{max} corresponded to the sine of the maximum local grain deviation in radians. The knot area ratio also required transformation to avoid generating negative UTS in the selected models. The *KAI*, or Knot Area Index, was created by exponential transformation of variable *KAR*. Therefore, the *KAI* value tended to zero as the *KAR* increased.

Table 2. Indicating Properties Included in the Candidate Models

Variable	Description
ρ_{12}	Density adjusted to 12% moisture content (kg/m^3)
MOE_{dyn}	Dynamic modulus of elasticity adjusted to 12% moisture content (N/mm^2)
SGD_{max}	Sine of the maximum local grain deviation in radians on the worst face of the lamella
$GD_{max1.5}$	Maximum grain deviation on the worst face of the lamella on a length equivalent to the width of the lamella (°)
$Combined\_SOG_{1.5}$	Average maximum grain deviation on the four faces of the lamella on a length equivalent to the width of the lamella (°)
$Combined\_SOG_{Span}$	Average slope of grain in the test span of the four faces (°)
KAI	Knot Area Index [$e^{(-0.1*KAR)}$]

When multiple models showed a comparable performance (*i.e.*, similar *AICc* values), a final model was built by multimodel inference, which is also known as model averaging. This approach, described by Mazerolle (2006), uses the Akaike weights of the

models to weight the estimates and standard errors (SE) of each parameter, which results in estimates and SE that consider the information of all relevant models. All selected models presented normally distributed errors and homogeneous variances. The interactions between the explanatory variables were dismissed.

RESULTS AND DISCUSSION

Results from the Tensile Strength Tests

The ultimate tensile strength and other relevant properties of the specimens tested in tension are shown in Table 3. The mechanical properties determined from the test campaign appeared slightly higher than those in the literature. For white ash, Jessome (1977) reported a mean MOE of 12,800 MPa (13,406 MPa when adjusted to 12% MC), whereas the declared MOE for yellow birch was 14,100 MPa (14,700 at 12% MC). The respective mean density values from Jessome (1977) are 690 kg/m^3 for white ash and 670 kg/m^3 for yellow birch. No data were available regarding UTS of the investigated species.

Table 2. UTS and Other Relevant Properties of the White Ash and Yellow Birch Lamellae Tested in Tension

Species	*n*	Mean Density (kg/m^3)	Density SD (kg/m^3)	Mean MC (%)	Median UTS (MPa)	Min. UTS (MPa)	UTS SD (MPa)	Mean MOE_{app} (MPa)	Min. MOE_{app} (MPa)
White ash	62	712.7	45.1	10.0	85.7	16.4	38.0	14,195	8,806
Yellow birch	55	717.9	41.3	11.0	95.3	19.6	32.8	15,254	11,035

Table 3. Ranking of the Candidate Models and Related Indicators for White Ash after Model Selection

Model ID	Explanatory Variables	K	*AICc*	Delta *AICc*	*AICc* Weight	Log-likelihood
14	p_{12} + MOE_{dyn} + SGD_{max} + *KAI*	6	533.42	0.00	0.69	-259.95
17	MOE_{dyn} + SGD_{max} + *KAI*	5	535.21	1.78	0.28	-262.07
16	p_{12} + SGD_{max} + *KAI*	5	540.17	6.74	0.02	-264.55
9	SGD_{max} + *KAI*	4	550.89	17.46	0.00	-271.09
13	SGD_{max} + $Combined\_SOG_{Span}$ + *KAI*	5	551.28	17.86	0.00	-270.11
15	p_{12} + MOE_{dyn} + $Combined\_SOG_{Span}$ + *KAI*	6	554.31	20.88	0.00	-270.39
4	SGD_{max}	3	565.80	32.37	0.00	-279.69
10	$GD_{max1.5}$ + *KAI*	4	566.72	33.30	0.00	-279.01
11	$Combined\_SOG_{1.5}$ + *KAI*	4	566.81	33.38	0.00	-279.05
8	*KAI*	3	585.38	51.95	0.00	-289.48
12	$Combined\_SOG_{Span}$ + *KAI*	4	586.36	52.94	0.00	-288.83
19	MOE_{dyn} + $Combined\_SOG_{Span}$	4	586.40	52.98	0.00	-288.85
5	$GD_{max1.5}$	3	588.46	55.03	0.00	-291.02
18	p_{12} + $Combined\_SOG_{Span}$	4	589.29	55.86	0.00	-290.29
6	$Combined\_SOG_{1.5}$	3	590.92	57.50	0.00	-292.25
2	MOE_{dyn}	3	618.39	84.96	0.00	-305.99
3	p_{12} + MOE_{dyn}	4	620.61	87.19	0.00	-305.95
7	$Combined\_SOG_{Span}$	3	628.96	95.54	0.00	-311.27
20	Intercept only	2	630.14	96.71	0.00	-312.97
1	p_{12}	3	630.36	96.93	0.00	-311.97

Results of the Model Selection Process

Table 4 shows the ranking of the candidate models for white ash after the model selection process based on the *AICc*. The best model for the prediction of white ash UTS was model 14 (*AICc* = 533.42, w_i = 0.69). This model included visually assessed variables, namely the maximum local grain deviation (SGD_{max}) and Knot Area Index (*KAI*) as well as the density and the dynamic MOE (MOE_{dyn}). The second-best model was model 17 (*AICc* = 535.21, w_i = 0.28), which included all variables from model 14, except the density. The third most performing model was model 16 (*AICc* = 540.17, w_i = 0.02), which included the density, SGD_{max}, and *KAI*. The multi-model inference allowed the calculation of model-averaged estimates and their corresponding standard error at a 95% confidence level for the three best performing models, as presented in Table 5.

Table 4. Model-averaged Estimates and 95% Confidence Level Standard Error of the Final Models for the Two Investigated Species

	White Ash		Yellow Birch	
Parameter	Model-averaged Estimate	SE	Model-averaged Estimate	SE
p_{12}	0.1141	0.0572	-0.1373	0.0596
MOE_{dyn}	0.0034	0.0011	0.0058	0.0013
SGD_{max}	-66.46	9.44	-59.31	12.15
KAI	42.78	8.60	23.20	9.59
Intercept	-29.86	45.65	79.68	46.04

Figure 2 shows the model-averaged predictions and unconditional 95% confidence intervals for the best-fit model parameters for white ash.

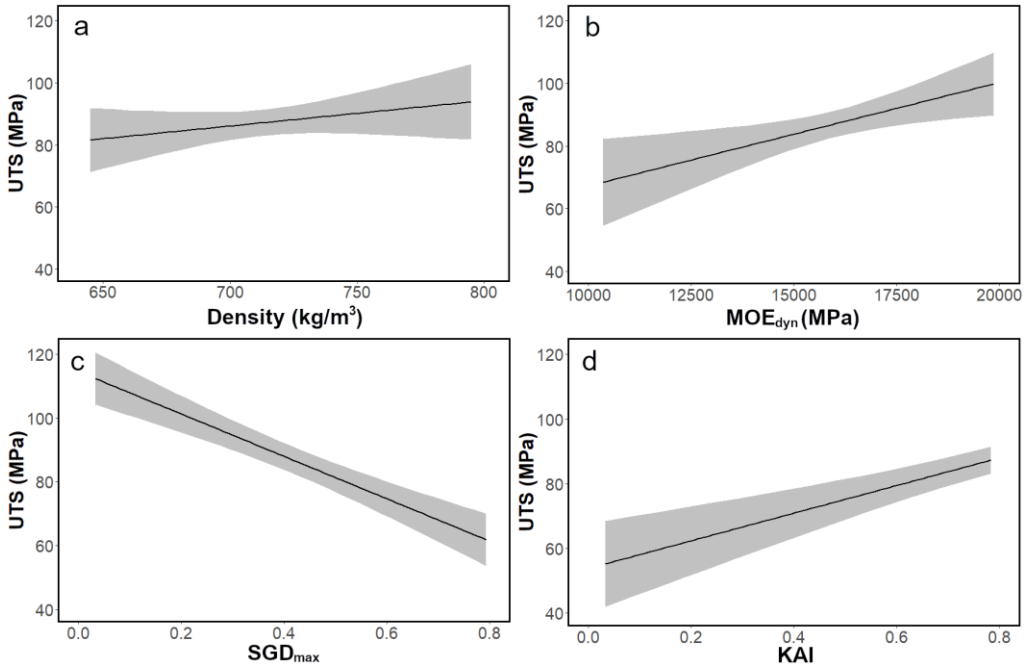

Fig. 1. The model-averaged predictions and unconditional 95% confidence intervals for the best-fit model parameters for white ash: a) Density; b) Dynamic modulus of elasticity; c) Sine of the maximum local grain deviation; d) Knot Area Index

The ranking of the candidate models for yellow birch is presented in Table 6. For this species, model 14 ($AICc$ = 459.83, w_i = 0.81) was the best model for predicting UTS. Model 17 ($AICc$ = 462.86, w_i = 0.18) was the second best model, followed by model 15 ($AICc$ = 468.88, w_i = 0.1), which included the density, MOE_{dyn}, KAI, and the combined average slope of grain in the test span (*Combined*_SOG_{Span}). However, the effect of *Combined_SOG*$_{Span}$ was not included in the final model because the maximum local grain deviation SGD_{max} was a stronger predictor of tensile strength.

Table 6. Ranking of the Candidate Models and Related Indicators for Yellow Birch After Model Selection

Model ID	Explanatory Variables	*K*	AICc	Delta AICc	AICc Weight	Log-likelihood
14	p_{12} + MOE_{dyn} + SGD_{max} + KAI	6	459.83	0.00	0.81	-223.02
17	MOE_{dyn} + SGD_{max} + KAI	5	462.86	3.03	0.18	-225.80
15	p_{12} + MOE_{dyn} + *Combined_SOG*$_{Span}$ + KAI	6	468.88	9.04	0.01	-227.54
9	SGD_{max} + KAI	4	475.35	15.52	0.00	-233.27
16	p_{12} + SGD_{max} + KAI	5	477.51	17.68	0.00	-233.13
13	SGD_{max} + *Combined_SOG*$_{Span}$ + KAI	5	477.74	17.91	0.00	-233.25
10	$GD_{max1.5}$ + KAI	4	477.78	17.94	0.00	-234.48
11	*Combined_SOG*$_{1.5}$ + KAI	4	480.11	20.28	0.00	-235.65
4	SGD_{max}	3	480.45	20.62	0.00	-236.99
19	MOE_{dyn} + *Combined_SOG*$_{Span}$	4	482.94	23.11	0.00	-237.06
5	$GD_{max1.5}$	3	484.80	24.97	0.00	-239.16
6	*Combined_SOG*$_{1.5}$	3	489.02	29.19	0.00	-241.27
18	p_{12} + *Combined_SOG*$_{Span}$	4	490.33	30.49	0.00	-240.76
8	KAI	3	497.91	38.08	0.00	-245.71
12	*Combined_SOG*$_{Span}$ + KAI	4	499.41	39.58	0.00	-245.30
3	p_{12} + MOE_{dyn}	4	505.49	45.66	0.00	-248.34
2	MOE_{dyn}	3	514.96	55.13	0.00	-254.24
1	p_{12}	3	529.51	69.68	0.00	-261.51
20	Intercept only	2	529.58	69.75	0.00	-262.67
7	*Combined_SOG*$_{Span}$	3	530.54	70.71	0.00	-262.03

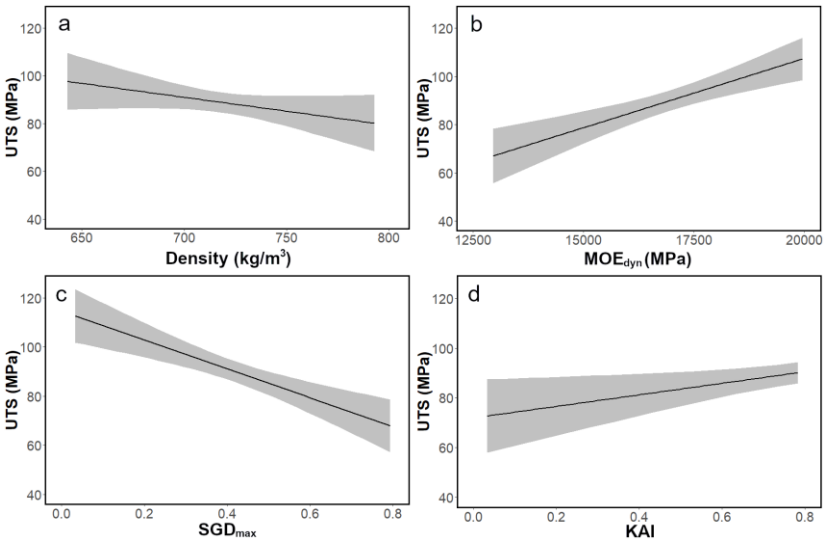

Fig. 3. The model-averaged predictions and unconditional 95% confidence intervals for the best-fit model parameters for yellow birch: a) Density; b) Dynamic modulus of elasticity; c) Sine of the maximum local grain deviation; d) Knot Area Index

The model-averaged estimates and their corresponding standard error at a 95% confidence level are presented in Table 5, and the model-averaged predictions plots for yellow birch are shown in Fig. 3.

Effect of the Explanatory Variables Included in the Final Models

The final models for white ash and yellow birch, despite showing similarities, exhibited major differences. The relationships between the mechanical and indicating properties were different for both species. Through isolating the effect of each of the explanatory variables included in the final models (Figs. 2 and 3), it was possible to better understand these differences and their implications for the grading of these species.

Effect of the density on the UTS

In this study, the density affected the two species differently, which is evident in the results in Table 5. Though the UTS of the white ash specimens increased as density increased, the opposite trend was observed for yellow birch. A deeper analysis of the test specimens revealed that the densest yellow birch lamellae that failed at a lower tension stress presented a wavy-grained pattern (Fig. 4) that was not visible on the other specimens. The presence of irregular grain patterns in yellow birch was well established, and it is generally undesirable except in some specific decorative products (Clausen and Godman 1967; Erickson and Ross 2005). Differences have already been observed between northern hardwood species regarding the effect of the density on their mechanical properties. In a study involving North American white ash, yellow birch, and sugar maple specimens, Kretchmann *et al*. (2010) concluded that the density changes affected the three species differently. Although their data suggested that strength increased as density increased, it was not possible to conclude definitively. In addition, higher density sometimes leads to lower mechanical properties. In a study on the grading of European hardwoods, Kovryga *et al.* (2019c) found a negative relationship between density and MOE for European maple.

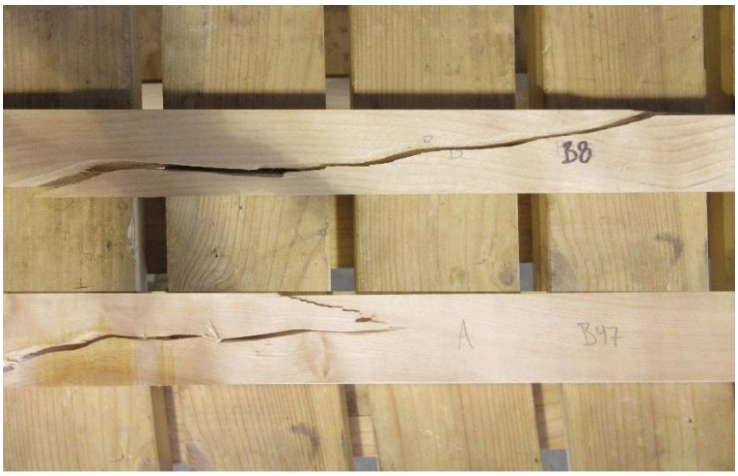

Fig. 4. Wavy-grained yellow birch specimens after failure

However, it is generally acknowledged that wood density has a direct and positive impact on the strength of both softwoods and hardwoods (Bendtsen and Youngs 1981; Ross 2010; Ravenshorst 2015). A study conducted on small, clear wood specimens from 160 hardwoods species and 32 softwood species revealed a coefficient of determination of 0.64 for the linear model relating the density to the bending strength of all species together

(Ravenshorst 2015). After subjecting small, clear wood specimens to bending tests, Zhang (1997) found R^2 values ranging from 0.50 to 0.74 between the density and MOR for four European birch and oak species. For structural timber, the effect of density is less obvious than it is for small, clear wood specimens. The variability in the properties of hardwood species reduces the accuracy of strength grading based on density (Frühwald and Schickhofer 2005; Brunetti *et al.* 2019; Kovryga *et al.* 2019b). Therefore, Ehrhart *et al.* (2016a) did not include this property in any of their candidate models. In this study, the generalized linear models in which the density was the sole predicting variable for UTS resulted in R^2 values of 0.015 for white ash ($p = 0.167$) and 0.024 for yellow birch ($p = 0.132$). Density, though not a good predictor in isolation, was still included in the best-performing models retained after the model selection process. In the first-ranked model (Model 14), the effect of the density was significantly correlated to the UTS ($p = 0.049$). The inclusion of additional indicating properties in the final models appeared to explain a larger proportion of the residual variance, which increased the significance of the density as a predictor of the UTS. These results, although different from initial expectations, were still consistent with findings from other studies on hardwood strength grading. When studying the relationship between the UTS and the density of European ash timber, Sarnaghi *et al.* (2017) obtained an R^2 of 0.006, whereas Kovryga *et al.* (2019c) found a slightly higher coefficient of determination ($R^2 = 0.034$) for the same species. Considering the results of the model selection process and the differences in the effect of the density on the UTS of the investigated species, this indicating property should be considered for the grading of white ash and yellow birch, unless its influence can be accounted for with other characteristics or indicating properties.

Effect of the grain deviations of the UTS

In this study, the generalized linear models in which the maximum local grain deviation was the only explanatory variable allowed the conclusion that this indicating property had a significant but limited impact on the UTS for both white ash ($R^2 = 0.05$, $p = 0.05$) and yellow birch ($R^2 = 0.07$, $p = 0.03$). It is well known that the angle made by wood fibres from the longitudinal axis of a lumber piece affects its bending strength. This effect can be approximated using the Hankinson equation (Bodig and Jayne 1982; Ross 2010; Ravenshorst *et al.* 2019), which is not linear. This non-linear relationship was also observed by Ravenshorst (2015) in a study on tropical hardwoods. In this study, the maximum local grain deviation had to be transformed to account for the non-linear relationship between the UTS and the maximum local grain deviation. In the models relating the grain deviations to the UTS, the substitution of the maximum local grain deviation with SGD_{max} considerably increased the portion of the UTS explained, as there was an R^2 of 0.65 ($p < 0.001$) for white ash and an R^2 of 0.62 ($p < 0.001$) for yellow birch. In softwood structural grading, the general slope of grain is often considered, and it is measured on a certain length and ignores the local grain deviations (Fruhwald and Schickhofer 2005; ASTM D245 2011). Due to the anatomical differences of hardwoods and their diversity, Sarnaghi *et al.* (2017) concluded that the grading methods for softwoods should not be applied for hardwoods. In this study, all the variables that expressed the general slope of grain were poor predictors of the tensile strength compared to the maximum local grain deviation expressed by SGD_{max}. The final models show that the relative importance of SGD_{max} as a predictor of UTS differed between white ash and yellow birch. The reduction in tensile strength caused by the maximum local grain deviation appeared to be of a larger magnitude for white ash, as there was an estimated reduction of

-66.46 for white ash compared to -59.31 for yellow birch. In a study of the impact of the slope of grain on the bending strength of white ash, yellow birch, and sugar maple, Kretschmann *et al.* (2010) came to a similar conclusion, suggesting that grain deviations had a bigger impact on the bending strengths of white ash and sugar maple than on that of yellow birch.

In addition, results from other studies on hardwood grading revealed a certain variability in the relationships between the grain angle and the bending or tensile strength. The main challenge in relating the grain deviations to the mechanical properties comes from the difficulty of visually assessing this property on sawn hardwood products (Fruhwald and Schickhofer 2005; Ravenshorst 2015; Bollmus *et al.* 2017), which depends on the species and evaluation method. Fruhwald and Schickhofer (2005) measured the grain deviations accurately on beech by considering the fracture pattern after testing, and they obtained a moderate correlation ($R^2 = 0.44$) with bending strength. However, Brunetti *et al.* (2019) found that neither the slope of grain measured visually or after failure was related to any of the mechanical properties of beech timber. Kovryga *et al.* (2019d) measured the slope of grain by transverse ultrasound on the worst 150 mm section of European ash and maple lamellae and concluded that neither transverse ultrasound measurement nor the slope measured after failure were significantly correlated with tensile strength. For European oak, Riesco-Muñoz and Remacha-Gete (2012) also found that the general slope of grain did not have a significant impact ($p > 0.05$) on the bending strength or MOE.

In this study, the high significance of SGD_{max} is attributable to the short span of the measurements but may have also been due to the limited cross section (38 mm × 38 mm) of the tested specimens, which resulted in a more accurate estimation of the real grain deviations. Stapel and van de Kuilen (2014) showed that visual grading techniques are strongly influenced by the cross section of the specimen, and some defects cannot be properly detected on larger cross sections. Nevertheless, it was feasible to measure the grain deviations visually for both investigated species. A considerable proportion of the specimens failed in the region where the worst local grain deviation was measured. The annual rings boundary method was the easiest way to measure the grain deviations, and the failure patterns (Fig. 5) confirmed the suitability of this method. However, this technique was only appropriate for specimens that presented an almost perfectly radial face. Grain deviations were more difficult to assess on the other specimens, and the process required more time. In addition, grain deviations were easier to measure visually on white ash than on yellow birch.

The results confirmed a statistically significant effect of the grain angle on the UTS. The maximum local grain deviation appeared to be a relevant indicating property for the strength grading of the investigated species. To accurately and efficiently measure the grain deviations of a greater diversity of cross sections and species, the measurement method must be refined, as the measures taken on larger specimens may be less reliable. To address this issue, Ehrhart *et al.* (2018) developed an automatic image analysis method for beech that calculates the grain deviations from the spindles formed by the medullary rays. This technique is also be applicable to other species. In a study on the strength grading of European ash and European maple, Kovryga *et al.* (2019d) found a strong correlation between the slope of grain measured by transverse ultrasound and the measure taken from the failure pattern. However, the deviation measured on a 150 mm length was not correlated with the tensile strength, but reduction of the measurement span may lead to better results. Similar methods could be applied to the species investigated in this study.

However, the prohibitive cost of some of these scanning technologies may limit their applicability in an industrial context (Erickson and Ross 2005).

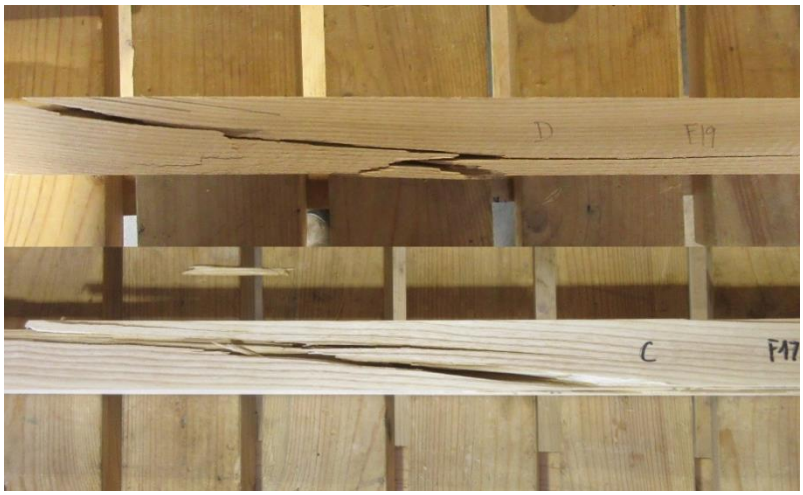

Fig. 5. The failure patterns following the ring boundaries on radially sawn white ash specimens

Effect of the modulus of elasticity on the UTS

The effect of the stiffness, accounted for by MOE_{dyn}, was comparable for both species. Increased stiffness improved the UTS, but the magnitude of the effect was larger for yellow birch, as shown by the higher model-averaged estimate for yellow birch than white birch (0.0058 and 0.0034, respectively). The coefficient of determination of the linear model relating MOE_{dyn} to the UTS was also higher for yellow birch ($R^2 = 0.28$, $p < 0.001$) than for white ash ($R^2 = 0.19$, $p < 0.001$). The modulus of elasticity is currently the main indicating property considered in machine grading, and its relationship with the bending strength is among the most documented. Experiments conducted by Smulski (1991) on small, straight-grained white ash, sugar maple, and white oak specimens revealed that the dynamic MOE was significantly ($p \leq 0.05$) correlated with the bending strength. Smulski also concluded, in line with the tensile strength results of this study, that the MOE explained a larger portion of the bending strength of yellow birch ($R^2 = 0.92$) than that of white ash ($R^2 = 0.85$). For hardwoods, the MOE is correlated to the tensile strength. However, the power of this indicating property is lower for temperate hardwoods ($R^2 = 0.38$) than for softwoods ($R^2 = 0.48$) and tropical hardwoods ($R^2 = 0.50$) (Ravenshorst 2015).

In structural timber, the introduction of strength-reducing defects reduces the portion of the strength variations explained by the MOE, which results in lower R^2 values. In a study of strength grading of European ash and European maple, Kovryga *et al.* (2019d) found a coefficient of determination of 0.62 between MOE and UTS, whereas Sarnaghi *et al.* (2017) found a slightly lower R^2 of 0.41 between the two variables for European ash. Further, Weidenhiller *et al.* (2019) reported an R^2 of 0.19 between tensile strength and dynamic MOE for European ash. However, the different span considered in both measurements would explain the weaker correlation. The prediction accuracy for tensile strength also depends on the quality of the material. Westermayr *et al.* (2018) reported an R^2 value of 0.48 between UTS and MOE for low quality beech, whereas Ehrhart *et al.* (2016b) reported an R^2 of 0.22 with high quality beech.

The dynamic MOE, as measured in this study, was found to be a reliable indicating property that should be included in strength grading procedures for the investigated hardwood species. However, considering the relatively low coefficients of determination (especially for white ash), other indicating properties should be included to reach satisfactory prediction accuracy.

Effect of knots on the UTS

In this study, knots were among the factors that most notably affected the UTS. The *KAR* measured on the specimens was transformed and expressed by the *KAI*, which prevented the model to generate negative UTS values. There was a direct and highly significant influence of *KAI* on the UTS, as there were R^2 values of 0.52 for white ash ($p < 0.001$) and 0.48 for yellow birch ($p < 0.001$). Figures 2 and 3 show that increasing *KAI* values resulted in a higher UTS because the *KAI* value increases as the dimension of the knot decreases. The results also indicated that the relative influence of the knots was considerably higher for white ash than for yellow birch, which was evident in their respective estimates (42.78 and 23.20) in the final models.

The results from this study were consistent with findings from other studies on hardwood species that concluded that the relationship between knots and UTS was existent but variable among species. When relating the largest knot parameter to the tensile strength, Fruhwald and Schickhofer (2005) found a coefficient of determination of 0.34 for European ash, beech, and oak species, whereas Ehrhart *et al.* (2016a) reported an R^2 of 0.53 between *KAR* and the UTS of European beech. Kovryga *et al.* (2019d) found an R^2 of 0.78 between *KAR* measured by transverse ultrasound and UTS. The coefficient of determination was only slightly lower ($R^2 = 0.74$) when considering the *KAR* measured visually.

The *KAR* (expressed here as *KAI*) should be included as an indicating property in grading procedures for the investigated species. However, for grain deviations, additional test campaigns are required to confirm the applicability of the results to larger cross sections. The impact of the position of the knot should also be assessed. In this study, no distinction was made between edge and centre knots. Knots located on the edge of a board affect bending strength depending if the knots are positioned on the tension or compression side of a lumber piece. Edge knots are also presumed to have a larger impact on tensile strength than knots located in the centre of boards, as their eccentricity induces additional stresses (Ross 2010).

Implications for the Strength Grading of the Investigated Species

The results from this study have confirmed several of the difficulties in hardwood strength grading, which are among the main factors limiting their use in structural engineered wood products (Schlotzhauer *et al.* 2019). However, the final models built from multimodel inference were satisfactorily accurate in predicting the UTS of both species using the selected indicating properties. In Fig. 6, the values predicted from the model-averaged estimates are plotted against the values obtained in the tests. The coefficients of determination of the linear models relating the actual UTS and model predicted UTS were 0.82 for white ash and 0.78 for yellow birch. As observed for the relationship between MOE_{dyn} and MOE_{app}, the coefficient of determination was slightly higher for white ash, which indicated that the mechanical properties of this species may be easier to predict than those of yellow birch.

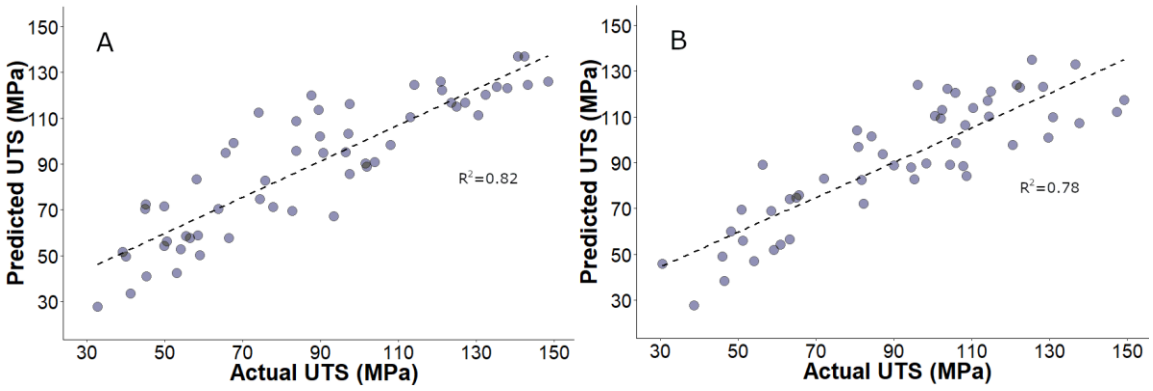

Fig. 6. The model-predicted and actual UTS results for white ash (A) and yellow birch (B) samples

The performance of the models developed in this study was comparable to the performance of commercially available machine grading systems for softwoods. With European spruce, Hanhijärvi and Ranta-Maunus (2008) reported R^2 values between 0.55 and 0.61 for the relationship between the UTS and the selected indicating properties, whereas the most advanced systems could lead to R^2 values above 0.70 between the indicating properties and the bending strength (Olsson *et al.* 2013). In addition, the prediction performance of the models from this study was comparable to that achieved in other studies on hardwood strength grading. Using 3D finite element numerical simulations, Sarnaghi *et al.* (2017) obtained a higher coefficient of determination (R^2 = 0.91) than that obtained in this study for the tensile strength prediction of European ash and European maple. Kovryga *et al.* (2019a) developed an automated grading system for European ash and European maple based on the MOE and the detection of knots by X-ray, which resulted in coefficients of determination of 0.58 and 0.53 for European ash and European maple, respectively.

The species investigated in this study presented some important differences in their behavior. The *KAI* and SGD_{max} variables more importantly affected the UTS of white ash, whereas the effect of MOE_{dyn} on UTS was more pronounced for yellow birch. The effect of increasing density was also opposite for the studied species. Because of interrelations between indicating properties and structural differences between hardwood species, it was difficult to determine the impact of density on hardwoods' strength in general. For instance, the density changes more importantly affected the stiffness of white ash and yellow birch than it did for sugar maple (Kretchmann *et al.* 2010). As the stiffness also impacts the bending and tensile strengths, these confounding effects are difficult to distinguish. Zhang (1997) also identified a statistically significant impact of density on the MOE of hardwood species, but this impact was of larger magnitude for ring-porous species than for diffuse porous species. In this study, some of the differences between the two species could be attributed to the fact that white ash is a ring-porous species, whereas yellow birch is a diffuse porous species. However, most of the differences were related to grain irregularities in yellow birch. This characteristic must be investigated to develop an accurate strength grading procedure for this species. A potential solution would be to define the presence of wavy grain as a criterion for exclusion. For instance, Riesco-Muñoz *et al.* (2011) suggested to systematically exclude European oak specimens presenting wavy grain because of their poor mechanical properties. However, before taking such action, the incidence of this characteristic and potential yield upon implementation of the restriction must be known.

Because wavy-grained specimens were also the densest, an abnormally high density could also serve as a criterion for exclusion.

Among the indicating properties included in the final models from this study, the grain angle was the most challenging to measure. The final models, including all four indicating properties, were more accurate in predicting the UTS than the other candidate models that were more parsimonious. However, for practical reasons, it may be necessary to simplify the grading procedure by removing indicating properties that are overly difficult to assess visually. For instance, Ravenshorst *et al.* (2019) suggested that the slope of grain should not be measured but rather considered indirectly from the MOE and density. The results from this study confirmed that both the maximum local grain deviation and SGD_{max} were significantly correlated with the dynamic MOE for yellow birch with respective p values of 0.037 and 0.029. However, for white ash, the p values of 0.069 for maximum local grain deviation and 0.052 for SGD_{max} were slightly over the desired significance level of 0.05. Further, candidate model 3, which included MOE_{dyn} and density as explanatory variables, was one of the worst performing models for both white ash ($AICc$ = 620.61, w_i = 0) and yellow birch ($AICc$ = 505.49, w_i = 0). Therefore, more research should be conducted on the accuracy of grain deviation measurements and the relationships between the grain deviations and other indicating properties. Other methods to assess the direction of wood fibers should also be investigated to improve the efficiency of the grading process.

The size effect of the specimens should also be investigated. As discussed earlier, the specimens tested in this study had uniform dimensions of 38 mm × 38 mm × 1830 mm. The conclusions presented in this study should be verified on larger cross section specimens. In addition, the probability of occurrence of strength-reducing defects increase as the cross section of the specimens increases (Weibull 1939; Pedersen *et al.* 2003). For European hardwoods, Schlotzhauer *et al.* (2017) were not able to conclude on the existence of a size effect on the tensile strength of the specimens. However, Kohler (2013) found that the tensile strength of spruce decreased as specimen length increased. These observations should be validated for white ash and yellow birch.

CONCLUSIONS

1. The ultimate tensile strength (UTS) of white ash and yellow birch lumber was successfully predicted from the density, dynamic modulus of elasticity, sine of the maximum local grain deviation (SGD_{max}), and knot area index (KAI). The final linear models resulted in coefficients of determination (R^2) between the actual and predicted UTS of 0.82 for white ash and 0.78 for yellow birch.
2. The final models revealed important differences between the two species, which indicated that it may be appropriate to grade them separately to ensure the most efficient resource utilization. The KAI and SGD_{max} more importantly affected the UTS of white ash than that of yellow birch, whereas the effect of the MOE on the UTS was more pronounced for yellow birch. The effect of increasing density was also opposite for the studied species.
3. Because of interrelations between indicating properties and differences in the mechanical behavior of both species, it was difficult to determine the impact of the density on the strength of hardwood timber. For instance, some wavy-grained yellow

birch specimens had an abnormally high density and failed at a lower tensile strength than expected.

ACKNOWLEDGMENTS

The authors are grateful to the Natural Sciences and Engineering Research Council of Canada for their support *via* the IRC and CRD programs (IRCPJ 461745-18 and RDCPJ 524504-18). In addition, the authors thank the Canada Graduate Scholarships-Master's (CGS M) program. Funding was also provided by the industrial partners of the NSERC Industrial Chair on Eco-responsible Wood Construction (CIRCERB) and the Fonds de recherche du Québec – Nature et technologies (FRQNT) scholarship Master's program. The authors are also grateful to the technical and undergraduate staff from the NSERC CIRCERB and the Renewable Materials Research Centre that contributed to the project.

REFERENCES CITED

Aicher, S., Christian, Z., and Dill-Langer, G. (2014). "Hardwood glulams – Emerging products of superior mechanical properties," in: *Proceedings of the World Conference on Timber Engineering 2014*, Quebec, Canada, pp. 287-296.

ASTM D245 (2011). "Standard practice for establishing structural grades and related allowable properties for visually graded lumber," ASTM International, West Conshohocken, PA, USA.

ASTM D1990 (2016). "Standard practice for establishing allowable properties for visually-graded dimension lumber from in-grade tests of full-size specimens," ASTM International, West Conshohocken, PA, USA.

ASTM D4761 (2013). "Standard test methods for mechanical properties of lumber and wood-base structural material," ASTM International, West Conshohocken, PA, USA.

Bendtsen, A., and Youngs, R. L. (1981). "Machine stress rating of wood: An overview," in: *Proceedings of the XVII IUFRO World Congress, Division 5*, Kyoto, Japan, pp. 21-34.

Bodig, J., and Jayne, B. A. (1982). *Mechanics of Wood and Wood Composites*, Van Nostrand Reinhold, New York City, NY, USA.

Bollmus, S., Gellerich, A., Schlotzhauer, P., Behr, G., and Militz, H. (2017). "Hardwood research at the Georg-August University of Goettingen," in: *Proceedings of the 6th International Scientific Conference on Hardwood Processing*, Lahti, Finland, pp. 116-122.

Brunetti, M., Nocetti, M., Pizzo, B., Aminti, G., Cremonini C., Negro, F., Zanuttini R., Romagnoli, M., and Scarascia Mugnozza, G. (2019). "Glued structural products made of beech wood: Quality of the raw material and gluing issues," in: *Proceedings of the 7th International Scientific Conference on Hardwood Processing*, Delft, Netherlands, pp. 230-242.

CEN EN 338 (2016). "Structural timber – Strength classes," European Committee for Standardization, Brussels, Belgium.

Clausen, K. E., and Godman, R. M. (1967). *Selecting Superior Yellow Birch Trees – A Preliminary Guide* (Research Paper No. NC-20), U.S. Department of Agriculture North Central Forest Experiment Station, St. Paul, MN, USA.

Ehrhart, T., Fink, G., Steiger, R., and Frangi, A. (2016a). "Strength grading of European beech lamellas for the production of GLT and CLT," in: *Proceedings of INTER Meeting Forty-Nine*, Graz, Austria, pp. 29-43.

Ehrhart, T., Fink, G., Steiger, R., and Frangi, A. (2016b). "Experimental investigation of tensile strength and stiffness indicators regarding European beech timber," in: *Proceedings of the World Conference on Timber Engineering*, Vienna, Austria, pp. 600-607.

Ehrhart, T., Steiger, R., and Frangi, A. (2018). "A non-contact method for the determination of fibre direction of European beech wood (*Fagus sylvatica* L.)," *European Journal of Wood and Wood Products* 76(3), 925-935. DOI: 10.1007/s00107-017-1279-3

Erickson, J. R., and Ross, R. J. (2005). *Undervalued Hardwoods for Engineered Materials and Components* (Report No. FPL-GTR-276), U.S. Department of Agriculture Forest Products Laboratory, Madison, WI, USA.

Frühwald, K., and Schickhofer, G. (2005). "Strength grading of hardwoods," in *Proceedings of the 14th International Symposium on Nondestructive Testing of Wood*, Eberswalde, Germany, pp. 198-210.

Galligan, W. L., and McDonald, K. A. (2000). *Machine Grading of Lumber – Practical Concerns for Lumber Producers* (Report No. FPL-GTR-7), U.S. Department of Agriculture Forest Products Laboratory, Madison, WI, USA.

Green, D. W., Ross, R. J., and McDonald, K. (1994). "Production of hardwood machine stress rated lumber," in: *Proceedings of the 9th International Symposium on Nondestructive Testing of Wood*, Madison, WI, USA, pp. 141-150.

Green, D. W., Winandy, J. E., and Kretschmann, D. E. (1999). "Mechanical properties of wood - Chapter 4," in: *Wood Handbook—Wood as an Engineering Material (FPL–GTR–113)*, U.S. Department of Agriculture Forest Product Laboratory, Madison, WI, USA.

Hanhijärvi, A., and Ranta-Maunus, A. (2008). "Development of strength grading of timber using combined measurement techniques: Report of the Combigrade Project—Phase 2," *VTT Publications* 686, 1-55.

Jessome, A. P. (1977). *Resistance and Related Properties of Native Wood Species in Canada*, Eastern Forest Products Laboratory, Ottawa, Canada.

Koehler, A. (1955). *Guide to Determining Slope of Grain in Lumber and Veneer*, U.S. Department of Agriculture Forest Products Laboratory, Madison, WI, USA.

Kohler, J., Brandner, R., Thiel, A. B., and Schickhofer, G. (2013). "Probabilistic characterisation of the length effect for parallel to the grain tensile strength of Central European spruce," *Engineering Structures* 56, 691-697. DOI: 10.1016/j.engstruct.2013.05.048

Kovryga, A., Schlotzhauer, P., Stapel, P., Militz, H., and Van de Kuilen, J.-W. G. (2019a). "Visual and machine strength grading of European ash and maple for glulam application," *Holzforschung* 73(8), 773-787. DOI: 10.1515/hf-2018-0142

Kovryga, A., Stapel, P., and van de Kuilen, J.-W. G. (2019b). "Mechanical properties and their interrelationships for medium-density European hardwoods, focusing on ash and beech," *Wood Material Science & Engineering* Online, 1-14. DOI: 10.1080/17480272.2019.1596158

Kovryga, A., Chuquin Gamarra, J. O., and van de Kuilen, J.-W. G. (2019c). "Machine strength and stiffness prediction with focus on different acoustic measurement

methods," in: *Proceedings of the 7th International Scientific Conference on Hardwood Processing*, Delft, Netherlands, pp. 211-219.

Kovryga, A., Sarnaghi, A. K., and van de Kuilen, J.-W. G. (2019d). "Strength grading of hardwoods using transversal ultrasound," in: *Proceedings of the 7th International Scientific Conference on Hardwood Processing*, Delft, Netherlands, pp. 220-229.

Kretschmann, D. E., Bridwell, J. J., and Nelson, T. C. (2010). "Effect of changing slope of grain on ash, maple and yellow birch bending strength," in: *Proceedings of the World Conference on Timber Engineering 2010*, Riva Del Garda, Italy, pp. 1014-1023.

Liu, Y., Gong, M., Li, L., and Chui, Y. H. (2014). "Width effect on the modulus of elasticity of hardwood lumber measured by non-destructive evaluation techniques," *Construction and Building Materials* 50, 276-280. DOI: 10.1016/j.conbuildmat.2013.09.029

Mazerolle, M. J. (2006). "Improving data analysis in herpetology: Using Akaike's Information Criterion (AIC) to assess the strength of biological hypotheses," *Amphibia-Reptilia* 27(2), 169-180. DOI: 10.1163/156853806777239922

Mazerolle, M. J. (2019). "AICcmodavg: Model selection and multimodel inference based on (Q)AIC(c), R package version 2.2-2," (https://cran.r-project.org/package=AICcmodavg), Accessed 12 Sept 2019.

Morin-Bernard, A., Blanchet, P., Dagenais, C., and Achim, A. (2020). "Use of northern hardwoods in glued-laminated timber: A study of bondline shear strength and resistance to moisture," *European Journal of Wood and Wood Products* Online, 1-13. DOI: 10.1007/s00107-020-01572-3

National Hardwood Lumber Association (NHLA) (2019). "Rules for the measurement and inspection of hardwood and cypress," National Hardwood Lumber Association, Memphis, TN, USA.

Niemz, P., and Mannes, D. (2012). "Non-destructive testing of wood and wood-based materials," *Journal of Cultural Heritage* 13(3S), S26-S34. DOI: 10.1016/j.culher.2012.04.001

Olsson, A., Oscarsson, J., Serrano, E., Källsner, B., Johansson, M., and Enquist, B. (2013). "Prediction of timber bending strength and in-member cross-sectional stiffness variation on the basis of local wood fibre orientation," *European Journal of Wood and Wood Products* 71, 319-333. DOI: 10.1007/s00107-013-0684-5

Panshin, A. J., and Zeeuw, C. D. (1970). *Textbook of Wood Technology Volume I: Structure, Identification, Uses, and Properties of the Commercial Woods of the United States and Canada*, McGraw-Hill, New York City, NY, USA.

Pedersen, M. U., Clorius, C. O., Damkilde, L., and Hoffmeyer, P. (2003). "A simple size effect model for tension perpendicular to grain," *Wood Science and Technology* 37(2), 125-140. DOI: 10.1007/s00226-003-0168-6

Ravenshorst, G. J. P. (2015). *Species Independent Strength Grading of Structural Timber*, Ph.D. Dissertation, Technische Universiteit Delft, Delft, Netherlands.

Ravenshorst, G., Gard, W. F., and van de Kuilen, J.-W. G. (2019). "Influence of slope of grain on the mechanical properties of hardwoods and the consequences for grading," in: *Proceedings of the 7th International Scientific Conference on Hardwood Processing*, Delft, Netherlands, pp. 169-175.

Ridley-Ellis, D., Stapel, P., and Baño, V. (2016). "Strength grading of sawn timber in Europe: An explanation for engineers and researchers," *European Journal of Wood and Wood Products* 74, 291-306. DOI: 10.1007/s00107-016-1034-1

Riesco-Muñoz, G., Remacha-Gete, A., and Pedras-Saavedra, F. (2011). "Implications in the design of a method for visual grading and mechanical testing of hardwood structural timber for designation within the European strength classes," *Forest Systems* 20(2), 235-244. DOI: 10.5424/fs/2011202-9771

Riesco-Muñoz, G., and Remacha-Gete, A. (2012). "Prediction of bending strength in oak beams on the basis of elasticity, density, and wood defects," *Journal of Materials in Civil Engineering* 24(6), 629-634. DOI: 10.1061/(ASCE)MT.1943-5533.0000428

Ross, R. J. (2010). *Wood Handbook: Wood as an Engineering Material* (FPL–GTR–190), U.S. Department of Agriculture Forest Products Laboratory, Madison, WI, USA.

Sarnaghi, A. K., Gard, W. F., and van de Kuilen, J.-W. G. (2017). "3D FE-numerical modelling of growth defects in medium dense European hardwoods," in: *Proceedings of the 6th International Scientific Conference on Hardwood Processing*, Lahti, Finland, pp.116-122.

Schlotzhauer, P., Nelis, P. A., Bollmus, S., Gellerich, A., Militz, H., and Seim, W. (2017). "Effect of size and geometry on strength values and MOE of selected hardwood species," *Wood Material Science & Engineering* 12(3), 149-157. DOI: 10.1080/17480272.2015.1073175

Schlotzhauer, P., Kovryga, A., Emmerich, L., Bollmus, S., van de Kuilen, J.-W. G., and Militz, H. (2019). "Analysis of economic feasibility of ash and maple lamella production for glued laminated timber," *Forests* 10(7), Article number 529. DOI: 10.3390/f10070529

Smulski, S. J. (1991). "Relationship of stress wave-and static bending-determined properties of four northeastern hardwoods," *Wood and Fiber Science* 23(1), 44-57.

Stapel, P., and van de Kuilen, J.-W. G. (2014). "Efficiency of visual strength grading of timber with respect to origin, species, cross-section, and grading rules: A critical evaluation of the common standards," *Holzforschung* 68(2), 203-216. DOI: 10.1515/hf-2013-0042

Weibull, W. (1939). "A statistical theory of the strength of material," in: *Proceedings of The Royal Swedish Institute for Engineering Research (No. 151)*, Stockholm, Sweden, pp. 1-45.

Weidenhiller, A., Linsenmann, P., Lux, C., and Brüchert, F. (2019). "Potential of microwave scanning for determining density and tension strength of four European hardwood species," *European Journal of Wood and Wood Prod*ucts 77, 235-247. DOI: 10.1007/s00107-019-01387-x

Westermayr, M., Stapel, P., and van de Kuilen, J.-W. G. (2018). "Tensile strength and stiffness of low-quality beech (*Fagus sylvatica*) sawn timber," in: *Proceedings of the World Conference on Timber Engineering 2018*, Seoul, South Korea, pp. 1-8.

Zhang, S. Y. (1997). "Wood specific gravity-mechanical property relationship at species level," *Wood Science Technology* 31, 181-191. DOI: 10.1007/BF00705884

Article submitted: August 4, 2020; Peer review completed: September 27, 2020; Revised version received and accepted: October 1, 2020; Published: October 9, 2020.
DOI: 10.15376/biores.15.4.8813-8832